

PHYSICAL REVIEW LETTERS

VOLUME 66

4 MARCH 1991

NUMBER 9

Realization of a Measurement of a “Weak Value”

N. W. M. Ritchie, J. G. Story, and Randall G. Hulet

Department of Physics and Rice Quantum Institute, Rice University, Houston, Texas 77251-1892

(Received 7 December 1990)

We present the first realization of a measurement of a “weak value,” a concept recently introduced by Aharonov, Albert, and Vaidman (AAV). Our experiment uses a birefringent crystal to separate the two linear-polarization components of a laser beam by a distance small compared to the laser-beam waist. This “weak measurement” is followed by a strong measurement which translates the centroid of the beam by a distance far larger than the birefringence-induced separation. In addition, we present data corresponding to orthogonal initial and final states, for which the weak value is not defined. This interference effect may have application in the amplification and detection of weak effects.

PACS numbers: 03.65.Bz, 42.10.Jd, 42.10.Qj

In a recent Letter, Aharonov, Albert, and Vaidman (AAV) introduced the concept of a “weak measurement.”¹ A weak measurement is one in which the coupling between the measuring device and the observable to be measured is so weak that the uncertainty in a single measurement is large compared with the separation between the eigenvalues of the observable.² Therefore, the eigenvalues are not resolved by the measuring device. In practice, there is necessarily some degree of uncertainty in any measurement. The “strength” of a measurement can be characterized on a continuous scale which extends from weak to ideal, depending on the measurement uncertainty relative to the eigenvalue separation. AAV show that under certain circumstances, a weak measurement of an observable A may produce surprising results. If prior to the weak measurement of the system is prepared in a state $|\Psi_i\rangle$ and afterwards, “postselected” to be in another state $|\Psi_f\rangle$, then the weak value of A may be defined as

$$A_w \equiv \langle \Psi_f | A | \Psi_i \rangle / \langle \Psi_f | \Psi_i \rangle. \quad (1)$$

A_w can be much larger than any of the eigenvalues of A , if $|\Psi_f\rangle$ is nearly orthogonal to $|\Psi_i\rangle$. The theory of this effect has been described in several recent publications.^{1,3-6} In addition to the fundamental interest of the weak-measurement concept, this procedure may be useful for the amplification and detection of weak effects.

Consider a system with an observable A with corresponding eigenvalues a_n and eigenstates $|A=a_n\rangle$. The

initial state of the system may be expanded in terms of the eigenstates of A as $|\Psi_i\rangle = \sum_n \alpha_n |A=a_n\rangle$. An ideal measurement of A has the following properties: (1) It always produces one of the eigenvalues a_n ; (2) the probability of the outcome a_n is $|\alpha_n|^2$; and (3) the system is left in the state $|a_n\rangle$ following a measurement result a_n . In a weak measurement, the eigenvalues are not fully resolved and the system is not left in an eigenstate of A , but rather in a superposition of the unresolved eigenstates. If an appropriate postselection is made, this superposition of eigenstates can coherently interfere to produce a “measurement” result A_w which is significantly outside the range of the eigenvalues of A . The postselection can be accomplished by making a strong measurement of some other observable B , and selecting one particular outcome. Thus, the final state is an eigenstate of B , which can be expressed as some linear combination of the eigenstates of A :

$$|\Psi_f\rangle = |B=b\rangle = \sum_n \alpha'_n |A=a_n\rangle. \quad (2)$$

The initial state can be prepared (or “preselected”) in a similar fashion.

AAV proposed an experiment which uses a beam of spin- $\frac{1}{2}$ particles to illustrate this effect. The initial and final states are selected by Stern-Gerlach magnets to be “spin up” along directions which are almost 180° apart. Therefore, $|\Psi_f\rangle$ and $|\Psi_i\rangle$ are nearly orthogonal. In between the preselection and postselection, a weak mea-

surement of the spin in a direction 90° relative to the postselection direction is performed. This is accomplished by a very weak Stern-Gerlach magnet in which the two spin orientations are deflected by an angle small compared with the divergence angle of the beam.

Our experiment is an optical analog of this spin- $\frac{1}{2}$ experiment which was recently proposed by Duck, Stevenson, and Sudarshan.³ In this analog, the beam of spin- $\frac{1}{2}$ particles is replaced by a Gaussian-mode laser beam and the preselection and postselection Stern-Gerlach magnets are replaced by optical polarizers. The weak measurement is performed by a birefringent-crystalline quartz plate which spatially separates the two orthogonal polarizations of the laser radiation by a distance which is much less than the Gaussian beam waist of the laser beam.

The laser radiation is assumed to be propagating in the z direction and to be linearly polarized at an angle α

with respect to the x axis. The electric-field vector of this radiation is described by

$$\mathbf{E}_i = E_0 \exp\left[-\frac{x^2 + y^2}{w_0^2}\right] (\cos\alpha \hat{\mathbf{x}} + \sin\alpha \hat{\mathbf{y}}), \quad (3)$$

where w_0 is the beam waist. The light is incident on a plane-parallel uniaxial birefringent plate whose optic axis is aligned with the x axis. The plane of the plate includes the x axis and is rotated from the y axis by an angle θ . The birefringent plate performs a weak measurement by spatially separating the two orthogonal linear-polarization components of the field, corresponding to the ordinary and extraordinary rays,⁷ by a distance a which is small compared to w_0 . In addition, the birefringent plate introduces a phase difference ϕ between the two rays due to a difference in optical path length between them. After emerging from the plate, the electric field (ignoring the amount of displacement due to refraction common to both polarization components) is

$$\mathbf{E}_w = E_0 \exp\left[\frac{-x^2}{w_0^2}\right] \left[\cos\alpha \exp\left[\frac{-(y+a)^2}{w_0^2}\right] e^{i\phi} \hat{\mathbf{x}} + \sin\alpha \exp\left[\frac{-y^2}{w_0^2}\right] \hat{\mathbf{y}} \right]. \quad (4)$$

The postselection is performed by a polarizer aligned at an angle β with respect to the x axis:

$$\mathbf{E}_f = E_0 \exp\left[\frac{-x^2}{w_0^2}\right] \left[\cos\alpha \cos\beta \exp\left[\frac{-(y+a)^2}{w_0^2}\right] e^{i\phi} + \sin\alpha \sin\beta \exp\left[\frac{-y^2}{w_0^2}\right] \right] (\cos\beta \hat{\mathbf{x}} + \sin\beta \hat{\mathbf{y}}). \quad (5)$$

The intensity of the transmitted light $I(y)$ detected along the y axis is proportional to $|\mathbf{E}_f(x=0)|^2$:

$$I(y) = I_0 \left[\cos^2\alpha \cos^2\beta \exp\left[\frac{-2(y+a)^2}{w_0^2}\right] + \sin^2\alpha \sin^2\beta \exp\left[\frac{-2y^2}{w_0^2}\right] + 2 \cos\phi \cos\alpha \cos\beta \sin\alpha \sin\beta \exp\left[-\frac{(y+a)^2 + y^2}{w_0^2}\right] \right], \quad (6)$$

where I_0 , the maximum incident intensity, is proportional to $|E_0|^2$. We assume that the birefringence-induced displacement a is much less than the beam waist w_0 , corresponding to a weak measurement. Also, we will set $\alpha = \pi/4$. When $\beta = \alpha$, $I(y)$ results from the constructive superposition of two Gaussian distributions separated by a distance small compared to their Gaussian widths. In this case, $I(y)$ is approximately a single, unshifted Gaussian. When the second (postselecting) polarizer is rotated to an angle $\beta = \alpha + \pi/2 + \epsilon$, with $\epsilon \ll 1$, the initial and final states are nearly orthogonal. In this case, the two Gaussians destructively interfere. If $\frac{1}{2} a/w_0 \ll \epsilon \ll 1$, the interference will produce a single Gaussian, the centroid of which is shifted by the weak value $A_w \approx \frac{1}{2} a \times \cot(\epsilon)$, which can be much larger than a .³ As ϵ approaches zero, the approximations made by AAV break down and A_w , as defined by Eq. (1), diverges. For $\epsilon = 0$, rather than a single shifted Gaussian, $I(y)$ has two peaks separated by approximately $2^{1/2} w_0$, with maximum intensity $I \approx (2e)^{-1} (a/w_0)^2 I_0$. Therefore, the birefringence-induced separation a is magnified in the result-

ing intensity distribution, but at the expense of reduced intensity.

Figure 1 shows the experimental setup schematically. The laser is a single-mode frequency-stabilized He-Ne laser operating at a wavelength of 633 nm. It has a collimated beam waist w_1 of 1.53 mm. Although the effect is most dramatic for $w_0 \gg a$, it was necessary, for reasons discussed below, to focus the laser beam to a small w_0 . Lens L_1 , with a focal length of 415 mm, focused the beam to a minimum beam waist $w_0 = 55 \mu\text{m}$.

The birefringent crystal Q is an X -cut (optic axis in the plane of the surface) crystalline quartz plate with a thickness d of 331 μm . The crystal is positioned approximately 25 mm before the focused-beam waist. It has a specified wave-front distortion of less than $\frac{1}{10}$ of a wavelength and a scratch/dig figure of 0/0. Since quartz is optically active for light propagating parallel to the optic axis,⁷ alignment of the optic axis with the x axis greatly simplifies the analysis of the displacement. In this orientation, a linearly polarized beam aligned along the x axis

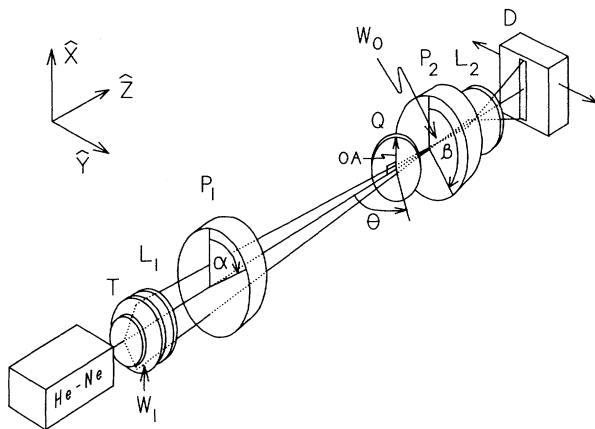


FIG. 1. Schematic diagram of the apparatus. The output of a frequency-stabilized He-Ne laser is collimated, focused, and polarized at an angle α relative to the x axis by telescope T , lens L_1 , and polarizer P_1 , respectively. A birefringent-crystalline quartz plate Q with optic axis (OA) aligned along the x axis is located near the focus of the laser beam. Q performs a weak measurement by spatially separating the ordinary and extraordinary polarization components by a distance small compared to the focused-beam waist w_0 . Polarizer P_2 , whose axis makes an angle β with the x axis, postselects the final polarization state. Lens L_2 expands the image onto a photodetector D . D is scanned along the y axis, recording the intensity function $I(y)$.

sees only the extraordinary index, $n_e = 1.55165$, while an orthogonally polarized beam sees only the ordinary index, $n_o = 1.54261$.⁸ Thus, the beam separation is given simply by Snell's law and geometry:

$$a = d \left[\frac{\sin(\theta - \theta_o)}{\cos(\theta_o)} - \frac{\sin(\theta - \theta_e)}{\cos(\theta_e)} \right], \quad (7)$$

where d is the crystal thickness, θ is the incident angle, $\sin(\theta_o) = \sin(\theta)/n_o$, and $\sin(\theta_e) = \sin(\theta)/n_e$. In this case, the Poynting vector and propagation vector are collinear. θ is adjusted to match the phase ϕ (modulo 2π) between the two different polarizations due to their different optical path lengths. We used $\theta \approx 30^\circ$, which gives $\phi/2\pi = 5$. Equation (7) then gives a displacement $a = 0.64 \mu\text{m}$.

Although the crystal faces are antireflective coated, a small fraction of the incident light undergoes multiple internal reflections and emerges from the crystal parallel to, but displaced from, the single-passed beam. As the beams diverge from the focus, this extraneous light intensity may overlap and obscure the interference pattern. Therefore, it was necessary to make w_0 small compared to d and, in addition, to use a lens L_2 (focal length = 10 mm) after Q to enlarge the image of the interference pattern on the image plane before this overlap occurs.

P_1 and P_2 are Glan-Thompson polarizers which are specified to produce a wave-front distortion of less than

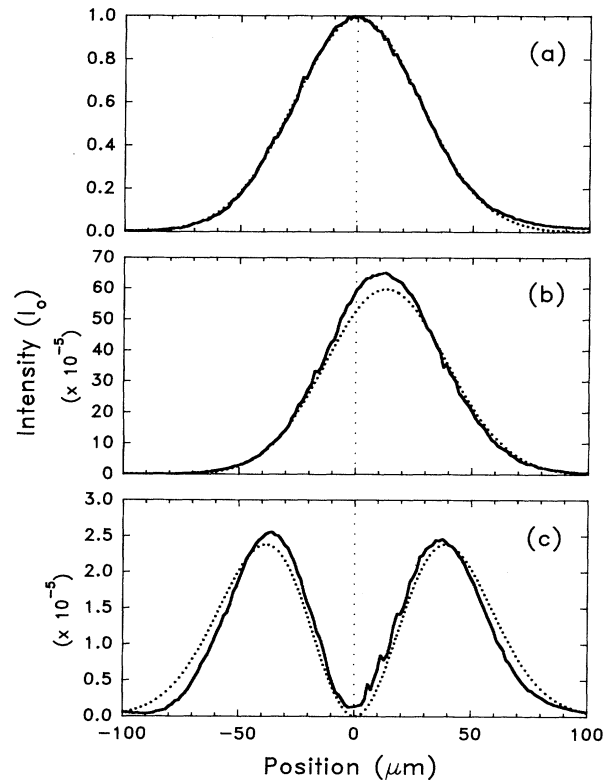


FIG. 2. Data and fits to the data using Eq. (6). The horizontal axis is scaled to measure y at the position of the focus of the laser beam. (a) $\alpha = \beta = \pi/4$, corresponding to aligned polarizers. The measured intensity profile is the result of the constructive addition of two approximately Gaussian distributions separated by a distance much less than the Gaussian beam waist. The dotted line, which almost perfectly overlaps the data, is a fit by a single Gaussian. (b) $\alpha = \pi/4$, $\beta = 3\pi/4 + 2.2 \times 10^{-2}$, corresponding to a measurement of the weak value. The resulting intensity is due to destructive interference of the two Gaussian distributions separated by a small distance $a \approx 0.64 \mu\text{m}$. The centroid of the distribution is shifted by $A_w = 12 \mu\text{m}$ or almost 20 times a . (c) $\alpha = \pi/4$, $\beta = 3\pi/4$, corresponding to crossed polarizers, or orthogonal initial and final states. In this case, A_w is undefined. The separation of the two peaks is ~ 120 times a .

$\frac{1}{10}$ of a wavelength. Measured as a pair, their extinction ratio is better than 1 part in 10^6 . Since the interference occurs at polarizer P_2 , the beam waist at P_2 , w_0 , is the critical dimension in determining the intensity of the interference pattern [Eq. (6)]. P_2 is located at the focus of L_1 to within our experimental uncertainty. Finally, the intensity profile is measured with a photodiode D located behind a $76\text{-}\mu\text{m}$ -wide slit. The photodiode-slit assembly is scanned across the y axis with a step size of $48 \mu\text{m}$.

Data and theoretical fits to the data using Eq. (6) are shown in Fig. 2. Figure 2(a) shows the resulting intensity distribution $I(y)$ for aligned polarizers, $\alpha = \beta = \pi/4$. In this case, the interference term in Eq. (6) (third term)

contributes constructively to $I(y)$. Since $a \ll w_0$, the profile is essentially a single Gaussian with a central intensity equal to I_0 . The dotted curve is a fit with a single Gaussian. We set the distance scale of Fig. 2 by taking this Gaussian width to be the measured beam waist, $w_0 = 55 \pm 4 \mu\text{m}$. The uncertainty is due to our uncertainty in the focus location of $\pm 5 \text{ mm}$. Figure 2(b) corresponds to the situation AAV call a weak measurement. In this case, $\alpha = \pi/4$ and $\beta = \alpha + \pi/2 + \varepsilon$ with $\varepsilon = 2.2 \times 10^{-2}$, so that the preselected and postselected polarization states are nearly orthogonal. The cross term in Eq. (6) now contributes a term similar in size to the first two terms but opposite in sign. Most of the intensity is canceled except for a small nearly Gaussian peak centered on the weak value, A_w . The data give $A_w = 11.9 \mu\text{m}$, which is ~ 19 times greater than a . Figure 2(c) corresponds to the case where the polarization axes of P_1 and P_2 are orthogonal ($\varepsilon = 0$). The interference term contributes destructively, causing an almost complete cancellation of the intensity. The remaining signal consists of two peaks which are nearly 5 orders of magnitude less intense than I_0 , and are separated by a distance much greater than a , approximately $2^{1/2}w_0$. The dotted lines in Figs. 2(b) and 2(c) are fits to the data using Eq. (6) with a as the only free parameter. The data of Fig. 2(b) give a best fit of $a = 0.65 \pm 0.05 \mu\text{m}$, while those of Fig. 2(c) give $a = 0.62 \pm 0.04 \mu\text{m}$, which agree well with the calculated value of $0.64 \mu\text{m}$. The uncertainty in the fit is due mainly to the uncertainties of w_0 and ε .

In conclusion, we have demonstrated the first realization of the measurement of a weak value. We have measured a weak value of the birefringence-induced displacement of a laser beam which is approximately 20 times larger than the actual displacement. Although we have demonstrated the phenomenon using an experiment which can be understood using classical physics, the principle is equally valid for quantum states. In our experiment, the initial and final states are the polarization states of the laser radiation. The eigenvalues of the weak measurement are the displacements of the beam, which are different for the two polarization states. The measurement is "weak" due to the smallness of this displacement compared with the size of the laser beam. Although the weak value A_w defined by Eq. (1) diverges when the initial and final states are orthogonal, as is the

case of the data of Fig. 2(c), the orthogonal condition is potentially useful for the amplification of very small effects. The separation between the two peaks of Fig. 2(c) is easily discernible by the naked eye and is ~ 120 times larger than the small birefringence-induced separation, which is comparable to the wavelength of light. We are unable to resolve this birefringence-induced separation in the data of Fig. 2(a). In fact, $a \approx 0.6 \mu\text{m}$ is less than the $1.4\text{-}\mu\text{m}$ separation between detector steps. In the crossed-polarizer case, the spatial amplification of a results in a significant loss of signal, since $I \propto (a/w_0)^2$. In this case, a precise measurement of a requires that the intensity be measured precisely, rather than the separation of the interference peaks which does not depend strongly on a .

The authors are grateful for the contributions of S. L. Keller and for helpful discussions with Professor P. M. Stevenson, Professor I. M. Duck, and Professor E. C. G. Sudarshan. This work was partially supported by the Texas Advanced Technology Program, the Robert A. Welch Foundation, and the NSF. R.G.H. is an Alfred P. Sloan Research Fellow.

¹Y. Aharonov, D. Z. Albert, and L. Vaidman, *Phys. Rev. Lett.* **60**, 1351 (1988).

²We use the term "measurement" in the same sense as AAV: A measurement is performed by the interaction of a system with a device which provides some information about the population of the eigenstates of an observable of the system.

³I. M. Duck, P. M. Stevenson, and E. C. G. Sudarshan, *Phys. Rev. D* **40**, 2112 (1989).

⁴See the following Comments: A. J. Leggett, *Phys. Rev. Lett.* **62**, 2325 (1989); A. Peres, *ibid.* **62**, 2326 (1989); and the Reply by A. Aharonov and L. Vaidman, *ibid.* **62**, 2327 (1989).

⁵Y. Aharonov and L. Vaidman, *Phys. Rev. A* **41**, 11 (1990).

⁶J. M. Knight and L. Vaidman, *Phys. Lett. A* **143**, 357 (1990).

⁷E. Hecht, *Optics* (Addison-Wesley, Reading, MA, 1987), 2nd ed.

⁸F. F. Martens, *Ann. Phys. (Leipzig)* **6**, 603 (1901). The indices n_e and n_o at 633 nm were calculated from the curves $n_o = 1.60324 - 1.585 \times 10^{-4}\lambda + 9.907 \times 10^{-8}\lambda^2$ and $n_e = 1.61258 - 1.581 \times 10^{-4}\lambda + 9.768 \times 10^{-8}\lambda^2$ which came from fitting Martens's values near 633 nm.